ICSV13 - Vienna
The Thirteenth International Congress on Sound and Vibration
Vienna, Austria, July 2-6, 2006

A COMPARATIVE STUDY OF FEATURE EXTRACTION METHODS FOR CRACK DETECTION IN ROTATING MACHINES OPERATING AT STEADY STATE

Yongxin Luo* and Steve Daley

Department of Automatic Control and Systems Engineering, University of Sheffield
Mappin Street, Sheffield, S1 3JD, United Kingdom
y.luo@sheffield.ac.uk

Abstract

Recent studies have evaluated the efficacy of various feature extraction methods in detecting rotor cracks using vibration signatures from machines undergoing transient operation. However, in many practical applications, rotating machines run at steady state for most of their operational life. This paper describes an investigation of a number of widely used feature extraction methods based on data obtained from a rotor running at steady state. The simulated cracked rotor utilises a simple hinge model together with a wide range of different crack depths which are represented by a change in stiffness. Based on the normal range of operating speed for rotating machines, the analysis is divided into two groups covering both the sub-critical and super-critical speed ranges. Rather than using visual discrimination or sophisticated comparison methodologies, simple statistics are adopted based on the extracted features. Measurement noise is also included for comparing the fault sensitivity of the various detection methods in relation to this. The main purpose of the study was to determine both the optimal operational speed and the optimal feature extraction method for crack detection.

INTRODUCTION

It is widely accepted that it is easier to detect cracks on rotors during the run-up or coast down stages of operation rather than at steady state ([2], [4]). A comparative study of feature extraction methods for crack detection on rotors during the run-up stage has been investigated by the authors in [3]. In that study, the methods underlined in Fig. 1 were systematically compared based on six different crack depths, and for both the noise free and the noise contaminated cases.

It will be noted, however, that rotating machines run at steady state for most of their operational life. So an investigation covering a rotor running at steady state is of great importance and may lead to a more practically viable method for online crack

Eds.: J. Eberhardsteiner, H.A. Mang, H. Waubke

detection. Nevertheless, regardless of the operating state, feature extraction, i.e. finding the most significant changes when a fault occurs, is the most important decision step. Several researchers have previously evaluated specific feature extraction methods for crack detection on rotors during stable operation. Examples include [1] where spectral analysis was applied for the steady state unbalance response of a Jeffcott rotor with a partially open and centrally located crack undergoing axial excitation; in [5] a crack detection method based on Wavelet time-scale contours obtained by the continuous Wavelet transform was proposed and evaluated using data from a steady state condition for a rotor with a transverse crack. As far as the authors of this paper are aware, a comparative study of the most widely used feature extraction methods for a cracked rotor operating in steady state is not available. Moreover, there does not appear to be a previous study that has investigated the noise effect on the various crack detection methods, even though noise may have a big or even crucial effect on detection. Therefore, a comparative study of feature extraction methods for crack detection on a rotor operating at steady state, for both noise free and noise contaminated signals is undertaken here. The analysis is individually carried out in the sub-critical speed region (at 0.2, 0.4, 0.6 and 0.8 times the first critical speed) and also for the super-critical speed range (at 1.2, 1.4, 1.6 and 1.8 times the first critical speed), in order to encompass the normal operating range of rotating machines.

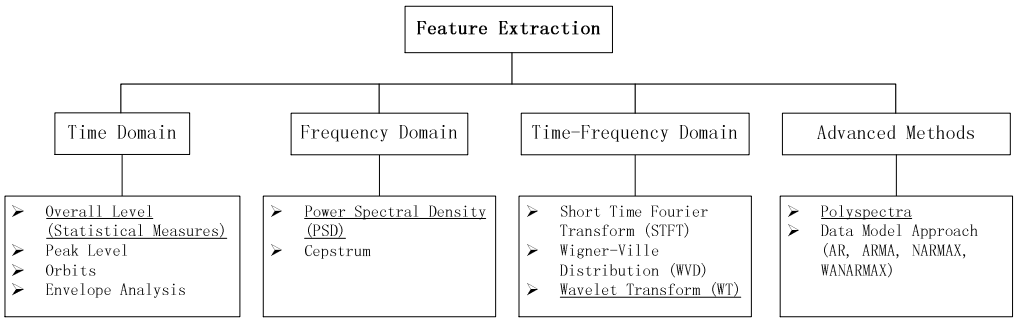

Fig. 1 - Feature Extraction Methods

MODELLING, SIMULATION AND PROCESSING

The development of a dynamic model and the numerical solution follows the approach presented in [2] and [5]. These papers model a De Laval rotor with a disk of mass m supported by a mass-less elastic shaft of length L, and assume that the crack is located near the disk at the mid-span of the shaft.

In the presence of a crack, the most significant additional deflection appears in the vertical direction of the rotating shaft. The shaft cross section is shown in Fig. 2 together with the co-ordinates used in the model. The resulting dynamic equation is

$$m\ddot{x} + c\dot{x} + k_x x = F_{ex} + F_0, \tag{1}$$

where m is the mass coefficient, c is the damping coefficient, and k_x is the stiffness coefficient.

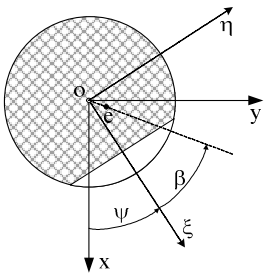

(x–y are stationary coordinates)

(ξ–η are rotating coordinates)

Fig. 2 - The cross section of a cracked rotor

The stiffness is described by

$$k_x = k - B\Delta k_\xi \cos^2 \psi, \tag{2}$$

where k is the stiffness of the un-cracked rotor; Δk_ξ is the stiffness variation due to cracks in one rotation direction; and $\psi = wt$, w is the angular speed. As the weight is assumed dominant, the Fourier series expansion of the rectangular function B representing the opening and closing or "Breathing" dynamic of the crack is

$$B = \tfrac{1}{2} + \tfrac{2}{\pi}\cos\theta - \tfrac{2}{3\pi}\cos 3\theta + \tfrac{2}{5\pi}\cos 5\theta - \cdots, \tag{3}$$

where $\theta = wt + \beta$, β is the angle between the eccentricity direction and the centric vertical direction of the crack. In equation (1), the excitation force F_{ex} and F_0 is

$$F_{ex} = me\ddot{\theta}\sin\theta + \dot{\theta}^2\cos\theta, \qquad \text{and,} \quad F_0 = mg, \tag{4}$$

respectively, where e is the eccentricity of the disk. Introducing dimensionless variables, equation (1) can be rewritten as

$$x_{\tau\tau}/x_{s\tau} + 2\zeta\, x_\tau/x_{s\tau} + x/x_{s\tau} - (B\Delta_{k_\xi}\cos^2(\Omega\tau))\, x/x_{s\tau} = \varepsilon\Omega^2\cos(\Omega\tau + \beta)) + 1, \tag{5}$$

where subscript τ and double subscript $\tau\tau$ denotes the first and second order derivative with respect to τ, $\tau = w_n t$; $x_{s\tau} = mg/k$ is the static deflection; $\zeta = c/2mw_n$ is the damping ratio; $w_n = \sqrt{k/m}$ is the natural frequency; $\Delta_{k_\xi} = \Delta k_\xi / k$ is the relative stiffness variation; $\varepsilon = e/x_{s\tau}$ is the relative eccentricity; and $\Omega = w/w_n$ is the relative angular speed. In order to simplify the analysis, the fourth term on the L.H.S. of equation (5) is normally approximated to $B\Delta_{k_\xi}\cos^2(\Omega\tau)$, as in [5] for example. It is argued here, however, that is not appropriate because the approximation will reduce the system nonlinearity introduced by the crack and thereby reduce fault sensitivity.

The simulated rotor comprises a 20mm diameter, 520mm length and 1kg steel shaft, and an 8kg mass disk at mid-span. The dimensionless parameters are: Ω = 0.2, 0.4, 0.6, 0.8, 1.2, 1.4, 1.6, 1.8, $\varepsilon = 0.1$, $\beta = 0$, Δ_{k_ξ} = 0, 0.003, 0.006, 0.009, 0.03, 0.06,

0.09 and $\zeta = 0.05$, respectively. The dynamic response, in this case the acceleration, is simulated by using a Runge-Kutta algorithm, and a data section with 1024 samples is obtained for each operating speed for the analysis. In the case of noise, the simulated data is contaminated by a relatively large independent uncorrelated noise with a signal to noise ratio (SNR) of 20dB relative to the vibration for $\Delta_{k_\xi} = 0$ and $\Omega = 0.8$.

The processing steps are summarized in Fig. 3, where CR denotes Change Rate, a simple statistic introduced here to enable a ready comparison between the relative detectability of different feature extraction methods, this is defined as:

$$CRn = \frac{\lambda_c - \lambda_0}{\lambda_0} \times 100\%, \qquad (n = 1, 2, \cdots 14) \tag{6}$$

where, λ_0 and λ_c are the statistical values (maximum, mean, RMS, …) of the extracted feature Λ obtained by using the signal processing methods in both the crack free and cracked case respectively. For time domain methods (TD), the feature Λ, the Kurtosis or RMS of time series, is a scalar value; for the Power Spectral Density (PSD), Λ is a magnitude vs. frequencies vector estimated by either the Periodogram or Pwelch method; for Bispectra (BSP), Λ is an amplitude or phase vs. frequencies vs. frequencies map estimated by the conventional direct approach; for Wavelet transform (WT), Λ is a magnitude vs. time vs. scales map obtained via Wavelet Packet.

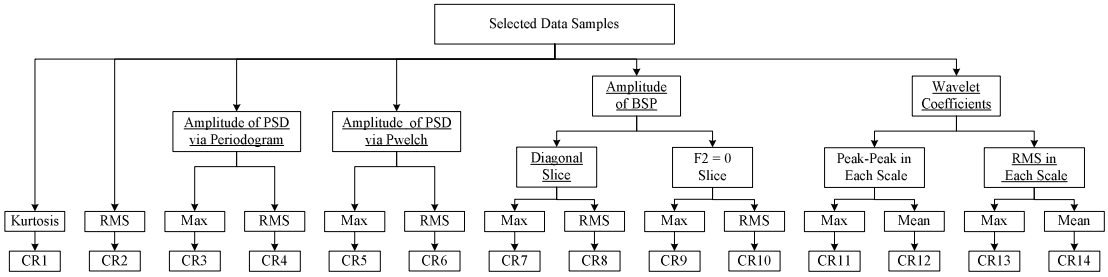

Fig. 3 - Feature extraction processing steps

RESULTS AND COMPARISON

The following analysis is made based on two groups: the sub-critical and super-critical speed ranges. It would be very useful to know at which particular operating speed the maximum detectability lies. The results shown in Fig. 5-8 are discussed below; Fig. 4 shows the plotting line styles and markers for the different features.

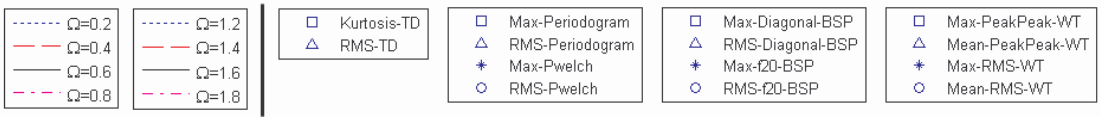

Fig. 4 – Plotting line styles (left) and markers (right) for different features

The kurtosis of time domain signal may not be able to detect cracks in this application because of the non-monotonic variation of its change rate with respect to

crack depth. This even loses detection functionality, as indicated by missing tags, at a sub-critical running speed (Fig. 5 - left), and the change rates are very small compared to the ones obtained from RMS in the super-critical speed range (Fig. 5 - right).

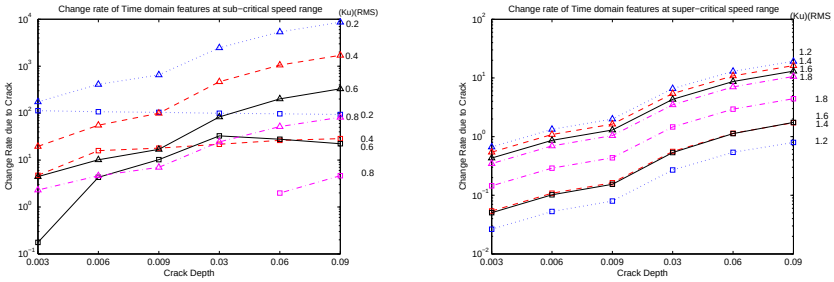

Fig. 5 - Change rates of TD at sub-critical speed (left) and super-critical speed range (right)

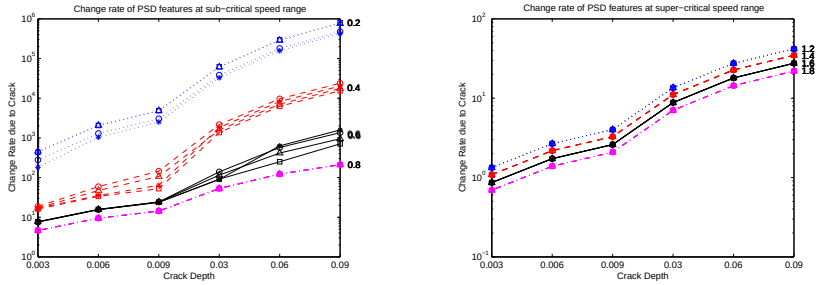

Fig. 6 - Change rates of PSD at sub-critical speed (left) and super-critical speed range (right)

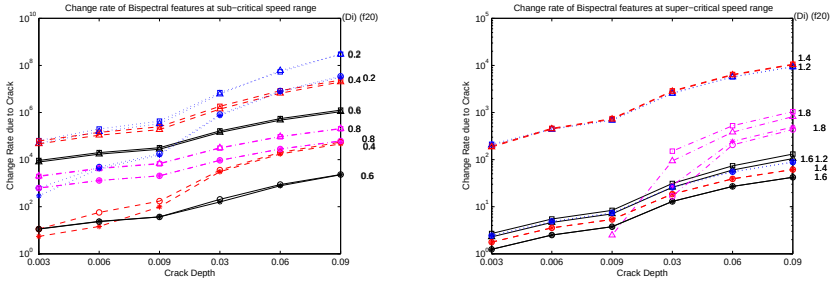

Fig. 7 - Change rates of amplitude of Bispectra at sub-critical speed (left) and super-critical speed range (right)

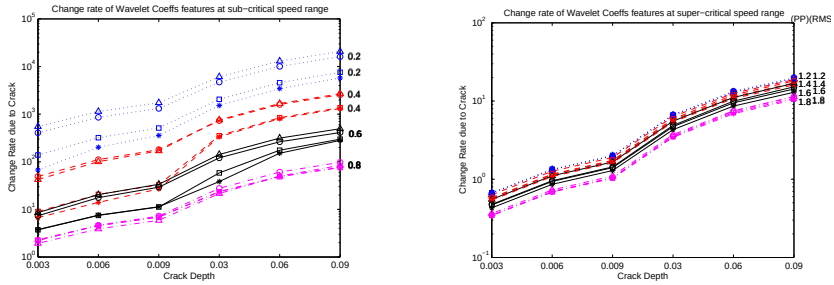

Fig. 8 - Change rates of Wavelet coefficients at sub-critical speed (left) and super-critical speed range (right)

Fig. 5 and 6 indicate that the change rates for the RMS of the time domain signal features and for the PSD features are clearly monotonically increasing with respect to both a crack depth increase and a running speed decrease, for both speed ranges. Fig. 7 and 8 show that the change rates of the statistics of the magnitude of Bispectra and the ones for the Wavelet coefficient features both increase as the crack depth increases. The variation of the change rates do not, however, universally follow the running speed, this is particularly true for the WT features for a small crack depth in the sub-critical speed range and for the f2=0 features of Bispectra in both speed ranges. Nevertheless, it can be seen that, in each speed range, the smaller the running speed, the better the fault detectability for the majority of the cases analysed.

A further analysis is carried out to investigate the different performance of the various features extraction methods, which are denoted by particular line styles and markers shown in Fig. 9. Fig. 10-13 indicate, that the statistics of features obtained by Bispectra, especially the diagonal slices, have much larger values of change rates than all other methods, although detectability is lost, as denoted by missing tags, when $\Omega = 1.8$; the change rates of the statistics of PSD are close to each other; the RMS of the time domain signal and the statistics of Wavelet coefficients have similar change rates in all speed cases, but they are smaller than the ones extracted by the PSD methods. Fig. 10-13 further prove that the Kurtosis may not be a good methodology in this application because it possesses the smallest change rates and even displays a non-monotonic variation with respect to the changing crack depth.

Fig. 9 – Plotting line styles and markers for different features

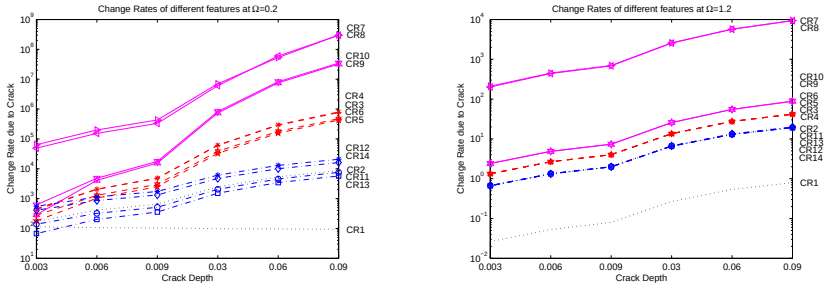

Fig. 10 - Change rates of different methods at $\Omega = 0.2$ (left) and $\Omega = 1.2$ (right)

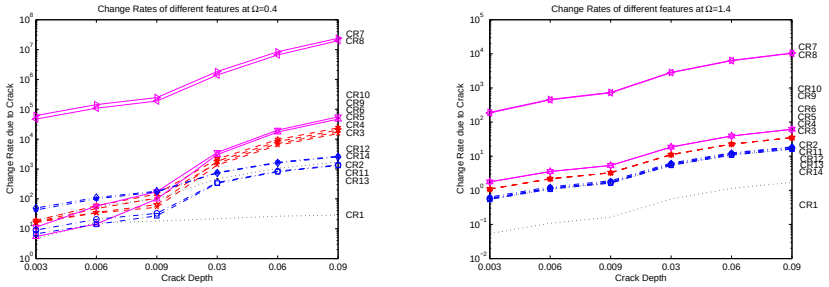

Fig. 11 - Change rates of different methods at $\Omega = 0.4$ (left) and $\Omega = 1.4$ (right)

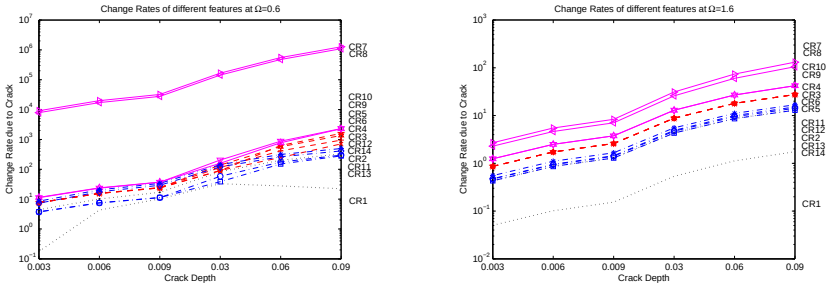

Fig. 12 - Change rates of different methods at $\Omega = 0.6$ *(left) and* $\Omega = 1.6$ *(right)*

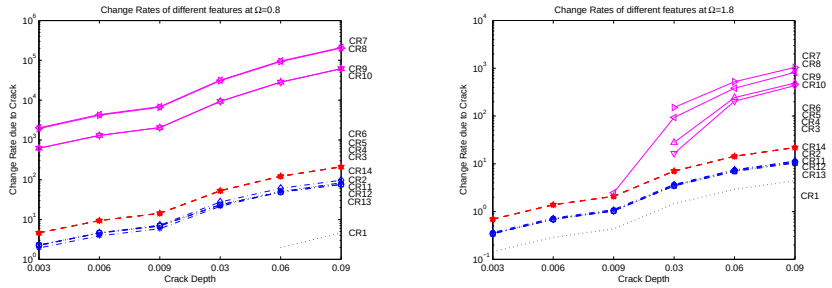

Fig. 13 - Change rates of different methods at $\Omega = 0.8$ *(left) and* $\Omega = 1.8$ *(right)*

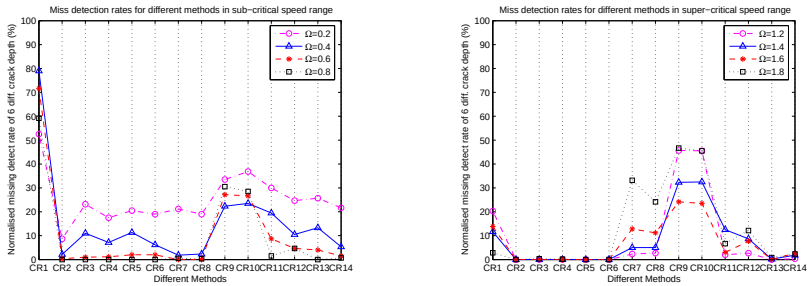

Fig. 14 - Missing detection rates for different methods in sub-critical (left) and super-critical (right) speed ranges

As a robustness indicator for the feature extraction methods, the missed detection rate was investigated based on six different crack depths (D1 to D6), eight different operating speeds ($\Omega = 0.2$ to $\Omega = 1.8$), and fourteen different methods (CR1 to CR14) contaminated by 100 groups of independent white noise each. Due to the page limit, only the sum of missed detection rates across each crack depth range (D1 to D6) is displayed, Fig. 14. The left figure clearly shows that, in the sub-critical speed range (except for f2=0 features of the Bispectra), the smaller the operating speed the bigger the missed detection rate. This is due to the small magnitude of the time domain signal at such speeds leading to a lower noise resistance. Although Kurtosis has small missed detection rates at super-critical speeds, Fig. 14(right), it has a high missed rate at sub-critical speeds. In both speed ranges, RMS of time domain signals and PSD features have the smallest missed detection rates when compared to all other methods, especially in the super critical speed case.

CONCLUSIONS

Several feature extraction methods for crack detection have been compared using data collected from a simulated rotor with six different crack depths and operating at two distinct steady state speed ranges. Both noise free and noise contaminated cases have been considered. The use of simple statistics of extracted features has been shown to provide an efficient measure of relative performance. For the noise free case, investigation shows that, generally, it is easier to detect a crack at the lower end of both operational speed ranges. Although it is difficult to be conclusive about which running speed enables maximum detection, it is clear that the Bispectra features provide the biggest overall fault sensitivity. The features extracted from time domain methods and the Wavelet transform provide the smallest change rate for the short period data section obtained from the simulated cracked rotor. For a signal to noise ratio of 20dB, the RMS of time domain signals and the PSD features possess very good noise resistance in both speed ranges. Investigation in the presence of noise has also shown that, when compared to all other methods the Bispectra features still possess the highest fault sensitivity (although missed detection rates are higher for a small crack depth). These conclusions are consistent with the authors' previous study on transient operation and demonstrate the feasibility of a more practical detection system that operates during steady state.

ACKNOWLEDGEMENTS

The authors gratefully acknowledge the financial support of ALSTOM Power Ltd and the technical advice of Dr Mark Donne and Dr Andrew Pike.

REFERENCES

[1] Darpe, A.K., *et al*., *"Analysis of the response of a cracked Jeffcott rotor to axial excitation"*, J. of Sound and Vibration, **249**, 3, 429-445 (2002)
[2] Gasch, R., *"Survey of the dynamic behaviour of a simple rotating shaft with a transverse crack"*, J. of Sound and Vibration, **160**, 2, 313-332 (1993)
[3] Luo, Y., S. Daley, *"A comparative study of feature extraction methods for crack detection"*, to be presented at the 6th IFAC Symposium on Fault Detection, Supervision and Safety of Technical Processes, Beijing, P.R.China, September, (2006)
[4] Sekhar, A. S., *"Crack detection through wavelet transform for a run-up rotor"*, J. of Sound and Vibration, **259**, 2, 461-472 (2003)
[5] Zou, J., *et al., "On the wavelet time-frequency analysis algorithm in identification of a cracked rotor"*, J. of Strain Analysis for Engineering Design, **37**, 3, 239-246 (2002).